FULL PAPER

Dalton
www.rsc.org/dalton

Nickel(II) and copper(II) complexes with pyridine-containing macrocycles bearing an aminopropyl pendant arm: synthesis, characterization, and modifications of the pendant amino group †

Aida M. Herrera,[a] Richard J. Staples,[b] Sergey V. Kryatov,[a] Alexander Y. Nazarenko *[c] and Elena V. Rybak-Akimova *[a]

[a] *Department of Chemistry, Tufts University, Medford, Massachusetts, 02155, USA*
[b] *Department of Chemistry, Chemical Biology, Harvard University, Cambridge, Massachusetts, 02138, USA*
[c] *Department of Chemistry, State University of New York, College at Buffalo, Buffalo, New York, 14222-1095, USA*

Received 20th November 2002, Accepted 6th January 2003
First published as an Advance Article on the web 3rd February 2003

The synthesis of three five-coordinate nickel(II) complexes with pendant arm-containing macrocycles has been achieved by the reduction of C=N bonds in the Schiff base precursors derived from diacetyl- or diformyl-pyridine and a tripodal tetramine. Demetallation of the nickel(II) macrocycles yielded stable pentadentate ligands that were used for the preparation of the copper(II) complexes. The structures of three nickel(II) complexes and two copper(II) complexes were determined by X-ray crystallography. Protonation of the pendant arm (pK_a = 6.3–6.6 for the nickel complexes, and 6.5–7.3 for the copper complexes) produced four-coordinate macrocycles, one of which was structurally characterized. The primary amino group of the pendant arm coordinated to the nickel(II) reacted with acetic anhydride or benzoyl chloride. The resulting mono-functionalized nickel(II) complexes and their copper(II) counterparts obtained by transmetallation displayed square-planar geometry in the solid state, as determined by X-ray crystallography, and remained four-coordinate in solutions below pH 11.

Introduction

Interest in macrocycles with pendant arms is growing on account of their unique coordination and structural properties, their utility in enzyme mimicking studies and catalysis, and their rapidly growing applications as radiopharmaceuticals, magnetic resonance imaging reagents, and fluorescent probes.[1–6] Biomedical applications of metallomacrocycles are often based on targeted delivery of the metal to specific cells or tissues, which requires covalent attachment of the macrocycle to a recognition moiety (usually, peptide or antibody). Immobilization of the macrocycles on solid supports is desirable in catalysis. Unambiguous single-point attachment is best accomplished *via* reactions with a functional group in the pendant arm.[5] The preparation of monofunctionalized macrocycles, however, is usually more elaborate than the synthesis of polyfunctionalized ligands (*e.g.*, through extensive alkylation of the secondary amino groups in azamacrocycles).[3,6] The development of simple methods for the preparation of monofunctionalized macrocyclic ligands that can be metallated with various transition metal ions is needed.

Pyridine-containing macrocycles are readily accessible and versatile platforms that give rise to a variety of structural motifs, including mono- and di-compartmental cycles, three-dimensional cages, sterically enforced macrocycles, and ligands with additional functional groups attached to the macrocycle.[7–10] The non-symmetric structure of these ligands allows for selective functionalization at non-equivalent amino group(s). We[11] and others[12–14] have previously reported a one-step synthesis of Schiff base macrocyclic complexes bearing a primary amino group in the pendant arm *via* a template condensation between diacetylpyridine and tripodal aliphatic tetramines. However convenient, these reactions are far from being universal, as their outcome depends on the nature of the metal template, and yields macrocyclic products with a limited selection of the metals (nickel(II) or copper(II)).[11] As metal-free Schiff base macrocycles derived from diacetyl- or diformyl-pyridine are notoriously unstable, transmetallation is hardly possible for these ligands. It is therefore desirable to modify the Schiff base complexes in such a way that stable free ligands would be accessible for future encapsulation of a variety of metal ions. Stable free ligands are also necessary for bioimaging and targeting with radioisotopes (*e.g.*, ^{67}Cu), where "hot" isotopes are added to the "cold kit" immediately before use.[15–17] Reduction of the azomethine bonds in pyridine macrocycles bearing a pendant arm was reported to yield stable compounds suitable for transmetallation.[18–23] The reactivity of the pendant arm, however, was not explored, in part because of the choice of pendant functional groups (such as tertiary amine, pyridine, or pyrazole) in the majority of known complexes.

This paper reports on the reduction of nickel(II) Schiff base macrocycles with a primary amino group in the "long" 3-aminopropyl pendant arm, and on their transmetallation with copper(II) (Scheme 1). Crystal structures of nine metal complexes are discussed. Two aspects of the chemistry of the pendant amino group are addressed: (1) "arm on"–"arm off" equilibrium upon protonation/deprotonation; (2) selective covalent modification of a coordinated amino group that yields a mono-acylated product.

Results and discussion

Synthesis and characterization

Template condensation of diacetylpyridine and a tripodal tetramine trpn in the presence of Ni(II) template in refluxing ethanol cleanly yields a target macrocyclic Schiff base complex $[Ni(L1a)]^{2+}$ (Scheme 1).[11] Although this reaction was previously run at high dilution in order to avoid formation of acyclic oligomers, we now found that the macrocycle remains a predominant product in more concentrated solutions (up to 0.03 M), so that the cyclization could be conveniently scaled up. Diformylpyridine undergoes similar template condensation at room temperature (the reaction is complete in 4 days), while

† Electronic supplementary information (ESI) available: colour versions of Figs. 4, 5 and 7. See http://www.rsc.org/suppdata/dt/b2/b211489e/

DOI: 10.1039/b211489e

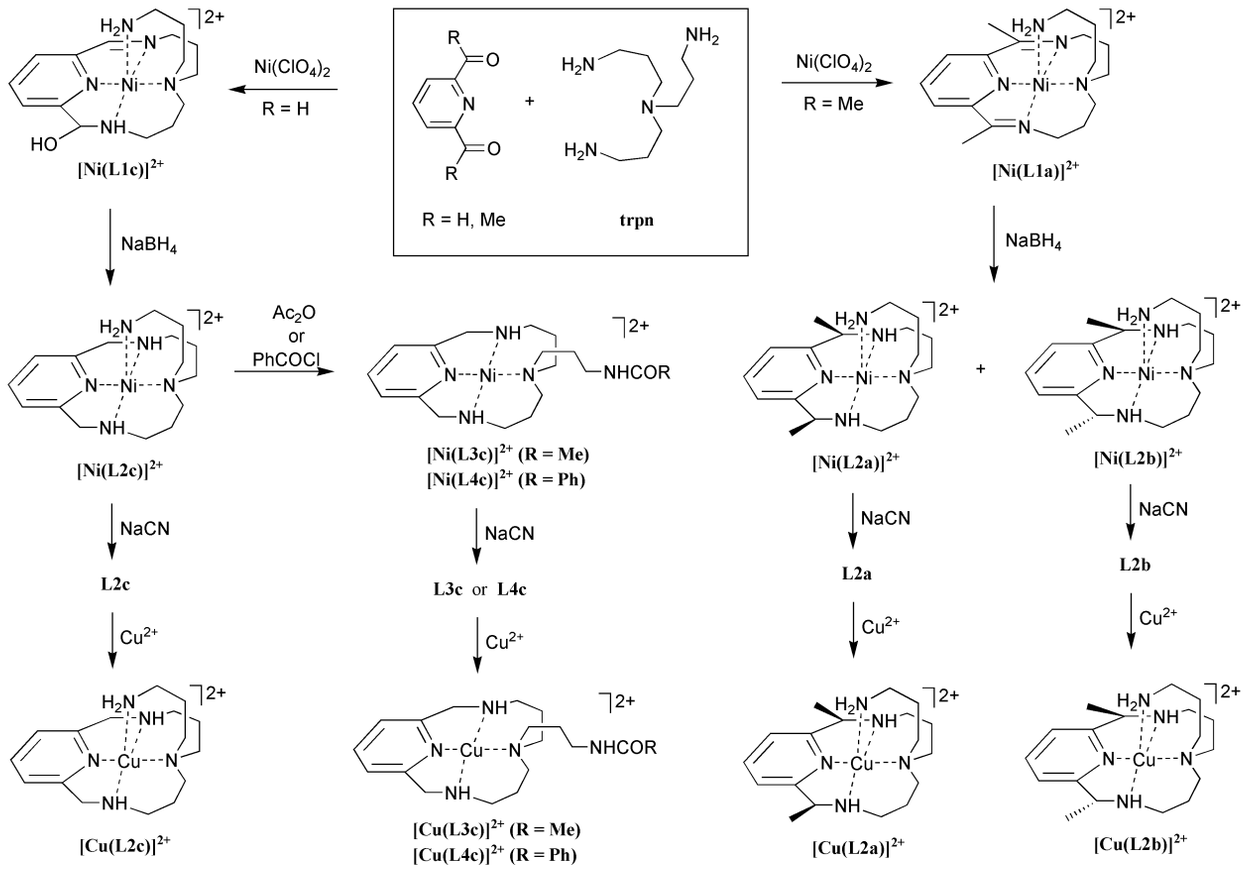

Scheme 1

heating the reaction mixture results in rapid irreversible degradation of the macrocycle (dark oligomeric products were not identified). The labile C=N bond(s) in macrocycles derived from diformylpyridine undergo rapid and reversible hydration, so that the crystallographically characterized monohydrate $[Ni(L1c)]^{2+}$ is the predominant component of the solid product.[24]

Reduction of $[Ni(L1a)]^{2+}$ and $[Ni(L1c)]^{2+}$ with an excess of sodium borohydride yields the corresponding aminomacrocycles (Scheme 1). Reduction proceeded smoothly when $NaBH_4$ is added all at once; the black precipitate that forms redissolves upon stirring. When $NaBH_4$ was added gradually, in small portions, incomplete reduction accompanied by contamination with non-cyclic products was observed. The reduced reaction mixture should not be left in solution for extended periods of time, as it gradually decomposes.

Reduction of the diformylpyridine derivative $[Ni(L1c)]^{2+}$ gave only one product that was identified as $[Ni(L2c)]^{2+}$. Therefore, facile and reversible hydration–dehydration of the unsubstituted Schiff base derived from diformylpyridine does not cause complications in the preparation of the reduced aminomacrocycle $[Ni(L2c)]^{2+}$. In the case of diacetylpyridine derivative $[Ni(L1a)]^{2+}$, hydration of the Schiff base was not observed under ambient conditions, but a different complication was expected. Reduction of $[Ni(L1a)]^{2+}$ generates two new stereocenters at the carbon atoms adjacent to the pyridine rings. Two different orientations of each of the methyl substituents with respect to the macrocyclic plane become possible, giving rise to *meso*- and *rac*-diastereoisomers of the free ligand. In metal complexes, two different orientations of the pendant arm also need to be considered, since the inversion of the coordinated tertiary nitrogen is expected to be very slow. Four stereoisomers of the reduced complex may exist that differ in relative orientation of the alkyl substituents (methyl groups or aminopropyl pendant arm) with respect to the macrocyclic plane (CH_3–CH_3–$C_3H_6NH_2$: up-up-up, up-up-down, up-down-up, down-up-up, with the last two structures being a pair of enantiomers). In practice, two major isomers of the nickel(II) complex were isolated from the reduced mixture by fractional crystallization (combined crystallization yield 94%). The isomers $[Ni(L2a)]^{2+}$ (blue) and $[Ni(L2b)]^{2+}$ (purple) give distinct electronic spectra and distinct NMR of the free ligands obtained by demetallation of the nickel(II) complexes (see Experimental). X-Ray crystallography revealed that the $[Ni(L2a)]^{2+}$ isomer has the up-up-up stereochemistry, and the $[Ni(L2b)]^{2+}$ isomer is a racemic mixture of the up-up-down and the down-up-up enantiomers (Scheme 1).

Isolated and purified purple or blue nickel(II) complexes with L2a–L2c were indefinitely stable in aqueous solutions. The identity and purity of the reduced complexes was confirmed by the IR (the absence of a C=N stretch at *ca.* 1640 cm^{-1}), mass spectrometry, elemental analysis, UV-Vis spectrophotometry (reversible spectral changes upon protonation/deprotonation of the pendant arm were indicative of the macrocyclic structures), and, in most cases, X-ray crystallography.

Nickel(II) complexes with L2a–L2c, when treated with an excess of NaCN, liberated macrocyclic ligands that could be isolated by extraction in chloroform or methylene chloride followed by solvent evaporation. Unlike their Schiff base precursors, these ligands were stable towards hydrolysis and could be used to prepare complexes of other metals. The free ligands were isolated as oily semi-solid materials, characterized by NMR and mass-spectrometry (see Experimental), and used without further purification.

Preparation of copper(II) complexes was straightforward: mixing the equivalent amounts of the ligand and copper(II) perchlorate in acetonitrile solution resulted in rapid and almost quantitative formation of the complexes $[Cu(L2a)]^{2+}$–$[Cu(L2c)]^{2+}$ that were isolated as perchlorate salts and crystallographically characterized.

Addition of one equivalent of a strong acid to copper(II) or nickel(II) complexes with L2a–L2c resulted in selective

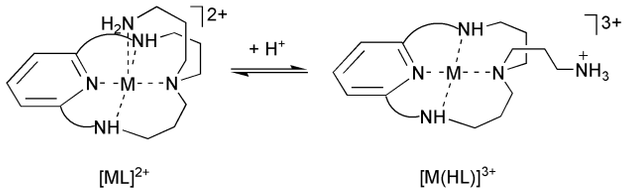

Scheme 2

protonation of the amino group in the pendant arm, as discussed in detail below (Scheme 2). A four-coordinate copper(II) complex $[Cu(HL2a)]^{3+}(ClO_4)_3$ was isolated and structurally characterized, confirming the dissociation of the pendant arm from the metal in the singly protonated complex.

Crystal structures

Three nickel(II) complexes and two copper(II) complexes with neutral ligands L2a–L2c were crystallographically characterized (Figs. 1–5, Tables 1 and 2). Although crystals of two of these materials ($[Ni(L2c)(ClO_4)_2]$ and $[Cu(L2a)](ClO_4)_2 \cdot CH_3CN$) were disordered, thus yielding somewhat less accurate metric parameters, the geometry of all complexes could be accurately determined. In all studied complexes with unmodified neutral ligands, the five nitrogen atoms are coordinated to the metal, resulting in a square-pyramidal geometry (four nitrogen donors of the macrocycle, N(1)–N(4), occupying the equatorial positions, and the nitrogen N(5) from the pendant arm being axial). No coordination of either the solvent molecules or anions was observed. A similar coordination geometry around the metal center was previously reported for analogous Schiff base[11,13] and reduced macrocyclic[21] copper(II) and nickel(II) complexes bearing a coordinating pendant arm attached at the N(3) nitrogen. Severe distortion of the aminopyridine macrocycle (folding along N(2)–N(4) axis), however, occurred upon coordination to copper(II) of a pendant group attached at the N(2) position.[25]

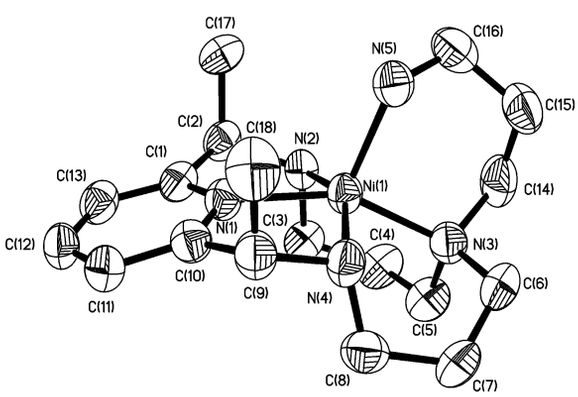

Fig. 1 ORTEP[67] plot of the complex $[Ni(L2a)](ClO_4)_2$. Perchlorate ions and hydrogen atoms are omitted for clarity.

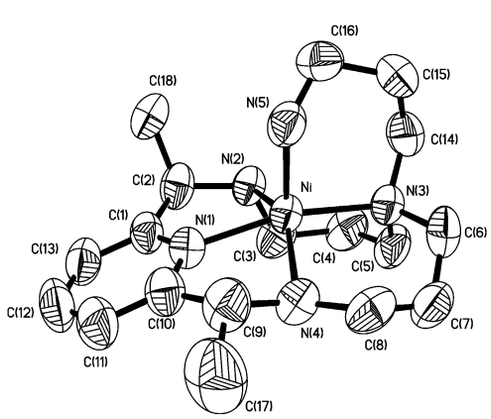

Fig. 2 ORTEP plot of the complex $[Ni(L2b)](ClO_4)_2$. Perchlorate ions and hydrogen atoms are omitted for clarity.

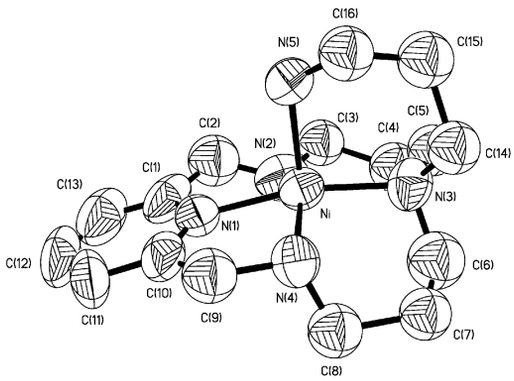

Fig. 3 ORTEP plot of the complex $[Ni(L2c)](ClO_4)_2$. Perchlorate ions and hydrogen atoms are omitted for clarity.

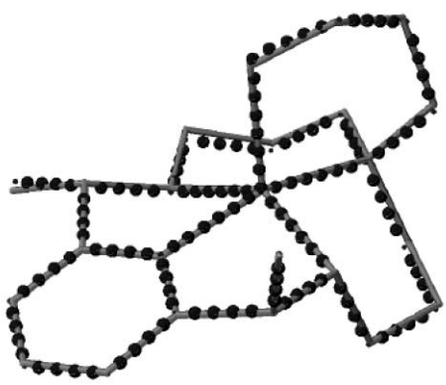

Fig. 4 Overlay of X-ray structures of $[Ni(L2b)]^{2+}$ (solid) and $[Cu(L2b)]^{2+}$ (dotted). The atom numbering scheme (identical for both complexes) is the same as that shown in Fig. 2.

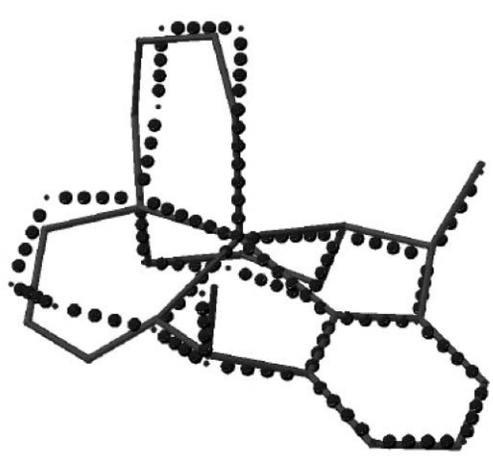

Fig. 5 Overlay of X-ray structures of $[Ni(L2a)]^{2+}$ (solid) and $[Cu(L2a)]^{2+}$ (dotted). The atom numbering scheme (identical for both complexes) is the same as that shown in Fig. 1.

Nickel–nitrogen distances in the five-coordinate complexes with L2a–L2c (1.94–2.17 Å, Table 1) are typical of high-spin Ni(II).[26] The shortest distance is between Ni(II) and the pyridine nitrogen N(1), followed by Ni–N(3) (tertiary amine *trans* to pyridine) and Ni–N(5) (primary amine in the pendant arm). The two remaining bonds to the secondary nitrogens N(2) and N(4) are slightly (in $[Ni(L2b)]^{2+}$) or significantly (in $[Ni(L2a)]^{2+}$ and $[Ni(L2c)^{2+}$) elongated, indicating trigonal distortion of the coordination polyhedron. As Ni(II) is shifted towards the pyridine ring, the N(1)–Ni–N(2) and N(1)–Ni–N(4) angles are less than 90°, and N(2)–Ni–N(3) and N(3)–Ni–N(4) angles are greater than 90°. Nickel is displaced from the macrocyclic plane

Table 1 Selected bond lengths (Å) and angles (°) in Ni(II) complexes

	$[Ni(L2c)](ClO_4)_2$	$[Ni(L2a)](ClO_4)_2$	$[Ni(L2b)](ClO_4)_2$	$[Ni(L3c)](ClO_4)_2 \cdot CH_3NO_2$
Ni(1)–N(1)	1.998(10)	2.002(5)	1.990(6)	1.835(5)
Ni(1)–N(2)	2.166(11)	2.115(5)	2.124(6)	1.937(5)
Ni(1)–N(3)	1.999(9)	2.057(5)	2.042(6)	1.953(5)
Ni(1)–N(4)	2.039(9)	2.133(5)	2.101(6)	1.941(5)
Ni(1)–N(5)	2.034(8)	2.019(5)	2.018(6)	—
Ni(1)–Other	—	—	—	2.799[a]
N(1)–Ni(1)–N(2)	76.6(5)	79.57(19)	79.5(2)	83.1(2)
N(1)–Ni(1)–N(3)	164.30(3)	151.12(19)	162.9(2)	177.0(2)
N(1)–Ni(1)–N(4)	82.6(4)	79.97(19)	78.5(3)	83.3(2)
N(1)–Ni(1)–N(5)	99.1(4)	110.9(2)	102.7(2)	—
N(2)–Ni(1)–N(3)	95.0(4)	94.20(19)	95.4(2)	95.3(2)
N(2)–Ni(1)–N(4)	146.6(4)	153.48(19)	145.4(3)	162.6(2)
N(2)–Ni(1)–N(5)	102.2(4)	105.62(19)	108.2(2)	—
N(3)–Ni(1)–N(4)	98.4(4)	95.61(19)	97.9(2)	97.8(2)
N(3)–Ni(1)–N(5)	95.6(4)	97.9(2)	94.4(2)	—
N(4)–Ni(1)–N(5)	106.8(4)	97.4(2)	102.5(3)	—
Metal displacement from N(1)N(2)N(3)N(4) mean plane	0.3855	0.4503	0.4167	0.1154

[a] Bonding to O of a ClO_4^- counterion of a different molecule.

Table 2 Selected bond lengths (Å) and angles (°) in Cu(II) complexes

	$[Cu(HL2a)](ClO_4)_3 \cdot CH_3CN$	$[Cu(L2a)](ClO_4)_2 \cdot CH_3CN$	$[Cu(L2b)](ClO_4)_2 \cdot 2C_3H_6O$	$[Cu(L3c)](ClO_4)_2$	$[CuL4c)](ClO_4)_2$
Cu(1)–N(1)	1.943(5)	1.975(3)	1.964(6)	1.936(5)	1.952(8)
Cu(1)–N(2)	2.039(4)	2.078(4)	2.080(7)	2.027(5)	2.026(8)
Cu(1)–N(3)	2.003(4)	2.032(3)	2.022(7)	2.010(5)	2.025(8)
Cu(1)–N(4)	2.035(5)	2.090(3)	2.077(6)	2.015(6)	2.033(8)
Cu(1)–N(5)	—	2.163(4)	2.167(7)	—	—
Cu(1)–Other	2.235[a]	—	—	2.485–2.596[b]	2.535[c]
N(1)–Cu(1)–N(2)	81.2(2)	78.78(14)	78.7(3)	82.6(2)	82.7(4)
N(1)–Cu(1)–N(3)	166.80(18)	160.40(14)	162.9(3)	179.4(2)	177.6(4)
N(1)–Cu(1)–N(4)	81.5(2)	80.19(13)	80.4(3)	82.2(2)	81.6(4)
N(1)–Cu(1)–N(5)	—	106.63(15)	103.9(3)	—	—
N(2)–Cu(1)–N(3)	96.5(2)	96.12(13)	97.2(3)	96.8(2)	97.4(3)
N(2)–Cu(1)–N(4)	155.3(2)	143.43(15)	143.7(3)	161.2(2)	159.7(4)
N(2)–Cu(1)–N(5)	—	106.79(15)	104.3(3)	—	—
N(2)–Cu(1)–N(6)	98.5(2)	—	—	—	—
N(3)–Cu(1)–N(4)	96.2(2)	93.79(13)	94.1(3)	98.3(2)	97.7(3)
N(3)–Cu(1)–N(5)	—	92.97(14)	93.3(3)	—	—
N(4)–Cu(1)–N(5)	—	107.74(16)	109.4(3)	—	—
Metal displacement from N(1)N(2)N(3)N(3) mean plane	0.2940	0.4627	0.4377	0.1052	0.1355

[a] Bonding to the N of a CH_3CN solvent molecule. [b] Bonding to O of a ClO_4^- counterion. [c] Bonding to O of a ClO_4^- counterion of a different molecule.

toward the pendant arm (separation from the mean N(1)N(2)-N(3)N(4) plane ranges from 0.39 to 0.45 Å), resulting in a decrease of the across-the-macrocycle bond angles (N(2)–Ni–N(4) and N(1)–Ni–N(3) are less than 180°). The values of the angular parameter of trigonal distortion, τ (which ranges from 0 for a perfect square pyramid to 1 for a perfect trigonal bipyramid)[27] are close to 0.3 for the majority of nickel complexes described in this paper.

The in-plane copper(II)–nitrogen distances (1.94–2.08 Å) are, on average, shorter than the corresponding distances in the nickel(II) complexes (Tables 1 and 2), which is consistent with the smaller radius of Cu^{2+}. The axial Cu–N(5) bond is significantly elongated (to 2.163 Å in the complex with L2a, and 2.167 Å in the complex with L2b) due to Jahn–Teller distortion. Copper(II) ion is also shifted toward the pyridine ring and displaced out of the macrocyclic plane (Table 2).

The conformations of the macrocycles L2a–L2c were very similar in all investigated complexes, except for $[Ni(L2a)]^{2+}$. In the latter complex, both hydrogen atoms at secondary amino groups (N(2) and N(4)) are pointed in the same direction as the pendant arm, and one of the six-membered chelate rings (Ni(1)N(3)C(6)C(7)C(8)N(4)) is forced to adopt a skewed conformation (Fig. 1). In the remaining four complexes, one of the NH vectors (at the N(2) atom) coincides with the direction of the pendant arm, while the other NH vector (at the N(4) atom) has the opposite direction (this hydrogen atom is located on the opposite face of the macrocyclic plane). All saturated six-membered chelate rings (two in the macrocyclic plane, and one formed by the pendant arm) adopt chair conformations. The similarity of the ligand conformations in copper(II) and nickel(II) complexes with L2b can be seen in the almost perfect overlay of the two structures (Fig. 4, root mean square deviations 0.0347 Å). In contrast, the copper(II) and nickel(II) complexes with L2a have a different configuration of the N(4) center, different conformations of the MN(3)C(6)C(7)C(8)N(4) chelate rings, and a somewhat different geometry of the pendant arm (Fig. 5, root mean square deviations 0.0506 Å).

Protonation of the coordinated pendant arm in the copper complex $[Cu(L2a)]^{2+}$ yields a complex $[Cu(HL2a)](ClO_4)_2 \cdot CH_3CN$, in which the four in-plane nitrogen atoms of the macrocycle are coordinated to the copper(II), while the protonated pendant amino group is no longer bound to the metal

Table 3 Pendant arm protonation constants and parameters of the electronic spectra of Ni(II) and Cu(II) complexes

Complex	pK_a	Solid state optical spectra[d]	Absorption bands, λ_{max}nm (ε/M^{-1} cm^{-1})[c]	
			pH 3.0	pH 10.0
Ni(L1a)[a]	6.46 ± 0.03			
Ni(L2a)	6.75 ± 0.04	378, 580, 800	472 (85)	368 (143), 571 (53) 812 (20), 885 (13)
Ni(L2b)	6.33 ± 0.03	361, 560, 822	465 (102)	362 (147), 562 (52) 829 (15), 885 (12)
Ni(L1c)	6.4 ± 0.1	—	460 sh (86), 570 sh (29), 800 sh (11)	534 (59), 801 (19) 920 (17)
Ni(L2c)	6.38 ± 0.03	335 sh, 553, 836, 884	464 (89)	352 sh (315), 559 (48), 823 (24), 885 (12)
Ni(L3c)	—	360 sh, 461	358 sh (233), 457 (110)[b]	
Cu(L1a)[a]	8.24 ± 0.06			
Cu(*iso*L1a)[a]	7.34 ± 0.04			
Cu(L2a)	6.5 ± 0.1	650, 926	579 (200)	628 (224), 888 (60)
Cu(L2b)	6.7 ± 0.1	640, 911	575 (187)	628 (229), 888 (67)
Cu(L2c)	7.3 ± 0.2	—	562 (187)	613 (229), 887 (67)
Cu(L3c)	—	—	556 (189)[b]	

[a] Ref. 11. [b] The spectra were measured at pH 7. [c] Determined in aqueous solutions at 25 °C. [d] Determined in Nujol mulls in absorbance mode.

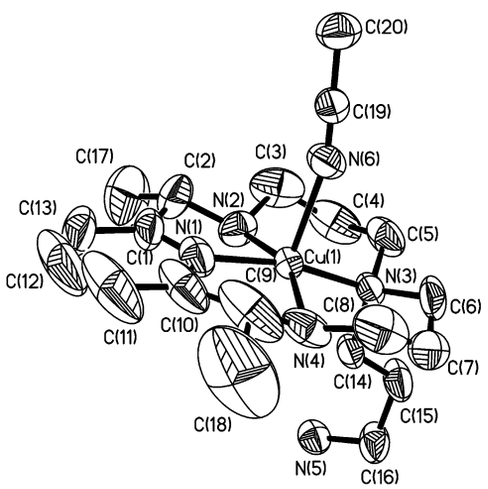

Fig. 6 ORTEP plot of the complex [Cu(HL2a)](ClO$_4$)$_3$. Perchlorate ions and hydrogen atoms are omitted for clarity.

(Fig. 6). The crystal structure of this complex is similar to the structures of copper(II) complexes with tetradentate aminopyridine macrocycles.[28–31] The Cu–N distances are now smaller than the Cu–N distances in the five-coordinate (non-protonated) precursor, as is the copper displacement out of the N_4 plane (Table 2). The copper(II) ion is located on the opposite face of the macrocycle with respect to the un-coordinated pendant arm. As a result, both NH vectors (at N(2) and N(4)) coincide with the pendant arm without disrupting chair conformations of the six-membered chelate rings of the macrocyclic complex. The macrocycle is substantially "flattened" as compared to the parent five-coordinate complex $[Cu(L2a)]^{2+}$. Interestingly, the fifth position is now occupied by the coordinated acetonitrile molecule (which binds opposite to the pendant arm). This situation is different from complex [Cu(L2a)]-(ClO$_4$)$_2$·CH$_3$CN, where all five nitrogens of the macrocycle were coordinated, and a non-coordinated acetonitrile filled the voids in the lattice.

Pendant arm protonation equilibria

The "long" aminopropyl pendant arm is coordinated to the metal (copper(II) or nickel(II)) in neutral or slightly alkaline solutions, but dissociates upon protonation in slightly acidic media. The aqueous solutions of $[NiL1]^{2+}$ become yellow upon adjusting pH to 3, and their electronic spectra are typical of low spin, square planar macrocyclic Ni(II) complexes, while purple or blue solutions of the complexes at pH 10 contain several low-intensity d–d transition bands with λ_{max} (*ca.* 370, 570, 800, and 900 nm) characteristic of the high-spin square-pyramidal $Ni^{II}N_5$ chromophore (Table 3).[11,32–34] Comparison of the UV-Vis spectra of the Ni(II) complexes in solid state and solution (Table 3) strongly suggests that the five-coordinate geometry found for the $[NiL1]^{2+}$ complexes in the solid state by X-ray crystallography is retained upon dissolving in water. It should be noted that high-spin five-coordinate complexes of Ni(II) are relatively rare.[11,23,26,32,33,35,36] Nickel(II) complexes with pentadentate ligands often pick up a counter-ion or a donor solvent molecule and become six-coordinate.[6,21,37,38]

"Arm-on" five-coordinate copper(II) complexes retain their square pyramidal geometry in solutions, as can be seen from the presence of two absorption bands in d–d spectra (at *ca.* 600 and 800–850 nm).[39] When the protonated pendant arm dissociates, square-planar complexes are formed, as evidenced by one strong-field transition in the electronic spectra. Both four-coordinate (protonated) and five-coordinate (non-protonated) complexes in frozen solutions give well-resolved axial EPR spectra with $g_{||} > g_{\perp}$ (see Experimental), indicating a $d_{x^2-y^2}$ ground state.[39] The spectral parameters reflect the usual increase of the equatorial ligand field in four-coordinate complexes *vs.* their five-coordinate counterparts.[39,40] The values of $g_{||}$ decrease from 2.207–2.210 in five-coordinate species to 2.187–2.192 in protonated, square-planar complexes, and the values of $A_{||}$ increase from (166–170) × 10^{-4} cm^{-1} in five-coordinate complexes to (193–202) × 10^{-4} cm^{-1} in protonated complexes upon dissociation of the pendant arm from the copper(II) center. Very similar UV-Vis and EPR spectral changes were observed for the Schiff base complexes with L1a,[11] and for other macrocycles bearing pendant arms.[18,41–43]

Quantitative data on the pH-dependent protonation of the pendant arm were obtained by spectrophotometrically monitored pH-titrations (Fig. 7). All reduced nickel(II) complexes

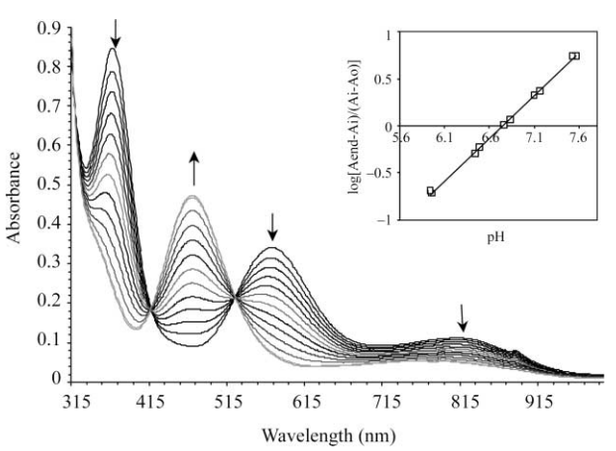

Fig. 7 UV-Visible spectrum of the arm on/off behavior of $[Ni(L2a)]^{2+}$. Concentration of initial [Ni(L2a)](ClO$_4$)$_2$ solution 0.006 M. The initial 2 mL of solution was titrated with 12 additions of 0.5 μL of 1.100 M HClO$_4$. The final acid concentration was 0.003 M.

showed completely reversible behavior over a broad pH range (3–11), and clear isosbestic points were present in UV-Vis spectra (Fig. 7). Equilibrium constants (Scheme 2) were calculated from the titration curves with high accuracy. The results for $[Ni(L1a)]^{2+}$ ($pK_a = 6.47 \pm 0.03$) agree perfectly with the pK_a value obtained previously by pH-potentiometric titrations (6.46 ± 0.03).[11] The Schiff base complex $[Ni(L1c)]^{2+}$ was less stable and partially decomposed upon prolonged titrations (especially in alkaline media). Copper(II) complexes with reduced macrocycles reacted with acid or base reversibly over a pH range from 3 to 8, but at higher pH, another process was observed (presumably, deprotonation of a coordinated water molecule) which was only partially reversible. This behavior somewhat limited the accuracy of pK_a determination for $[Cu(L2c)]^{2+}$, because deprotonation of the pendant arm in this complex occurred at relatively high pH, and no clear saturation of the titration curve was reached. The pK_a data are summarized in Table 3.

The protonation constants for pendant amino groups coordinated to metal ions in $[M(L2a)]^{2+}$–$[M(L2c)]^{2+}$ are relatively high, falling in the same pK_a range (6–8) as the protonation constants for aminopropyl pendant arm attached to isocyclam copper(II) and nickel(II) complexes.[42] Shorter side arms, which form five-membered chelate rings with the central metal ion, are usually less susceptible to protonation and dissociate from the metal in acidic media (pH ≈ 2).[18,21,23,42,43] The pH range for the proton-dependent dissociation of the coordinated aminopropyl arm is very convenient as it allows for switching between two different ligand binding modes under mild conditions. Weak coordination is also favorable for covalent modification of the primary amino group in the macrocyclic complexes, as discussed below.

The structure of the macrocycle (double *vs*. single C–N bonds and methyl substituents) exerts little effect on the pK_as of nickel(II) complexes (Table 3). The protonation constants of the pendant arms cluster around $pK_a = 6.4 \pm 0.0.1$ for all complexes except for $[Ni(L2a)]^{2+}$ that has somewhat higher pK_a value of 6.75 ± 0.04. The lower affinity of Ni(II) for pendant arm coordination in $[Ni(L2a)]^{2+}$ can be attributed to steric hindrance between the arm and two axial methyl groups facing the same side of the macrocycle. Such steric interactions are absent in the rest of our nickel(II) complexes: diformylpyridine derivatives L1c and L2c lack methyl groups, Schiff base macrocycle L1a contains methyl groups that are coplanar with the ring and would not interfere with the arm coordination, and complex $[Ni(L2b)]^{2+}$ has only one methyl substituent in the same configuration as the metal-bound aminopropyl arm.

The protonation constants of the copper(II) complexes depend on several factors and do not show one straightforward trend. Unlike protonated nickel(II) complexes that are square-planar, the analogous copper(II) "arm-off" macrocycles tend to bind solvent molecules in the axial positions. A coordinated acetonitrile molecule was found in the X-ray structure of $[Cu(HL2a)](ClO_4)_3 \cdot CH_3CN$ (Fig. 6). Notably, this solvent molecule is located at the opposite face of the ring with respect to the methyl and aminopropyl substituents. It appears that the axial methyl groups may screen the central copper(II) ion from the solvent coordination, thus facilitating pendant arm binding. Another important factor is the steric strain of the macrocyclic ligands in square-pyramidal five coordinate copper(II) complexes that could be partially relieved upon arm dissociation. This factor appears to be of particular importance for the rigid Schiff base complexes with the mismatch between the size of the ring and the radius of the copper(II) ion.[11] Although the flexible reduced ligands L2a–L2c can better accommodate copper(II), the L2a ligand changes conformation (and configuration of one of the macrocyclic NH-groups) upon proton-induced dissociation of the pendant arm (Figs. 4 and 6). It is difficult to quantify this effect in the absence of structural data for all "arm on" and "arm off" copper(II) complexes under investigation. The experimental data show that the pendant aminopropyl groups of the diacetylpyridine derivatives L2a and L2b have higher affinity for copper(II) than their diformylpyridine counterpart L2c (Table 3). The relatively high pK_a of $[Cu(L2c)]^{2+}$ resembles the high pK_a values previously found for Schiff base copper(II) complexes.[11]

Covalent modification of the coordinated amino group

Protonation studies of $[ML1]^{2+}$ and $[ML2]^{2+}$ demonstrated that two distinct metal binding sites with very different affinities for the metal ion are present in the pentadentate ligands. The aminopropyl pendant arm coordinates weakly and dissociates upon protonation at pH 6–8, while the macrocycle remains strongly bound to the metal even under acidic conditions. This observation suggests that the coordinated amino groups may display distinctly different reactivity with respect to covalent modification. Selective modification of the pendant amine would be beneficial for conjugation of the metallocomplexes to biomolecules,[44–46] or for fluorescent labeling of the complex.[47–49] Because coordination to the metal ion decreases nucleophilicity of the amino group, the modification of the free ligand followed by metal insertion into the macrocycle remains the most popular strategy for pendant arm functionalization.[44,45,48,49] Recently, direct functionalization of the metal complexes was reported,[45–47] where either non-coordinated[45,46] or weakly coordinated[47] amino group appended to the macrocycle or cage reacted with an electrophilic agent (dansyl chloride, chloroacetic acid, *etc*.). A particularly attractive feature of these reactions is the protecting role of the metal ion: metal coordination prevented extensive modification of the secondary amino groups of the macrocycles. Inspired by recent successes in derivatizing metallomacrocycles bearing an amino group, we decided to investigate the acylation of $[Ni(L2c)]^{2+}$. This strategy for selective amide bond formation would be useful for bioconjugation. Numerous possible applications of metal-assisted amide bond formation within the coordination sphere were previously explored in peptide synthesis,[50–55] ranging from protecting the amino group,[50,52] to activating the carbonyl component,[51,53,54] to templating the preparation of cyclic tetrapeptides.[55] Consequently, amide formation from coordinated peptide precursors is possible, even though the amino group is deactivated in metallocomplexes.

In reactions of the complex $[Ni(L2c)]^{2+}$ with acetic anhydride or benzoyl chloride, the amide was cleanly formed in the pendant arm, but no modification of the macrocyclic backbone was observed, as evidenced by mass spectrometry and NMR (Scheme 1). The acetylated product $[Ni(L3c)](ClO_4)_2$ was isolated and fully characterized as a low-spin, square-planar nickel(II) complex. The amide group in the long pendant arm did not coordinate to the metal ion up to pH 11, in agreement with the expected decrease in binding affinity of the pendant arm due to an increase in the length of a flexible linker. Kimura *et al*. found that an amide in a "short" pendant arm ($–CH_2C(O)NH–$) coordinates to the central zinc(II) ion, while a longer arm separated from the macrocycle by a C_2-linker did not bind.[56] Transmetallation of the acylated macrocyclic complex proceeded uneventfully (NaCN followed by Cu^{2+}, Scheme 1, Experimental) and yielded the corresponding copper(II) complexes $[Cu(L3c)]^{2+}$ and $[Cu(L4c)]^{2+}$ that were crystallographically characterized.

The coordination environments of copper(II) in the acetylated complex $[Cu(L3c)](ClO_4)_2$ (Fig. 8) and in the benzoylated complex $[Cu(L4c)](ClO_4)_2$ (Fig. 9) are very similar to that found in the singly protonated complex $[Cu(HL2a)](ClO_4)_3 \cdot CH_3CN$ (Fig. 6). Again, short in-plane Cu–N distances (from 1.936 to 2.027 Å, Table 2) are observed, with the axial position being occupied by a weak ligand (an oxygen of a perchlorate anion). The macrocycle is essentially undistorted, having both six-membered chelate rings in a chair conformation. The copper(II)

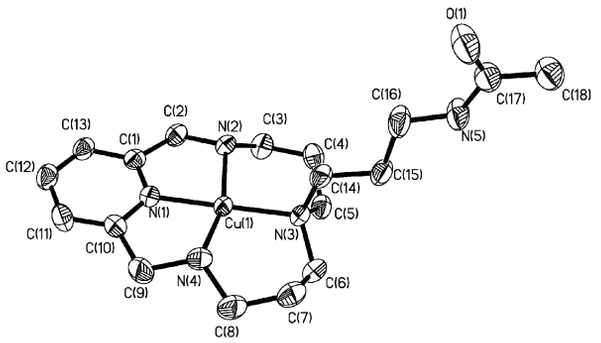

Fig. 8 ORTEP plot of the complex $[Cu(L3c)](ClO_4)_2$. Perchlorate ions and hydrogen atoms are omitted for clarity.

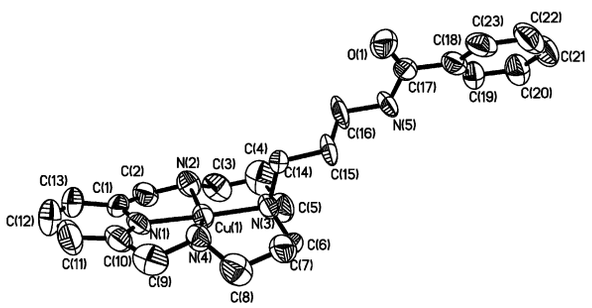

Fig. 9 ORTEP plot of the complex $[Cu(L4c)](ClO_4)_2$. Perchlorate ions and hydrogen atoms are omitted for clarity.

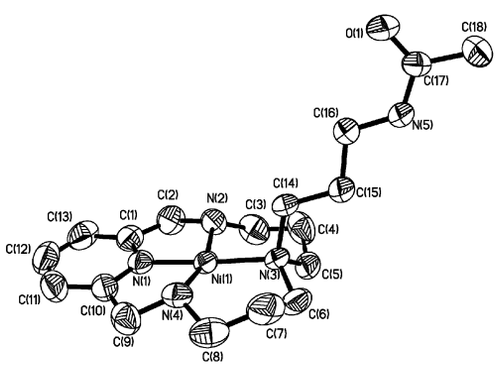

Fig. 10 X-Ray structure of $[Ni(L3c)](ClO_4)_2$. Perchlorate ions and hydrogen atoms are omitted for clarity.

ion is displaced down the N4 mean plane by only 0.105 Å, and the NH groups are parallel to the uncoordinated pendant arm. The corresponding nickel(II) complex, $[Ni(L3c)](ClO_4)_2$, contains a low-spin, four-coordinate metal in a square-planar environment (Fig. 10) with a relatively long separation from the oxygen atom of ClO_4^- (2.799 Å). All Ni–N distances are substantially shorter than those observed in the high-spin, five-coordinate complexes, and range from 1.835 to 1.953 Å. These distances are also shorter than the corresponding Cu–N distances in the complex cation $[Cu(L3c)]^{2+}$ (Tables 1 and 2). Due to uniform in-plane Ni–N bond lengths (only the Ni–N(1) bond to a pyridine nitrogen is shorter by 0.1 Å), and small Ni(II) out-of-plane displacement (0.11 Å), the bond angles approach their ideal values (90 or 180°). The conformation of the macrocycle in $[Ni(L3c)]^{2+}$ is identical to that of its copper counterpart.

As expected, the structures of modified copper(II) and nickel(II) complexes with a non-coordinated, N-acylated pendant arm closely resemble the structures of the Cu(II) and Ni(II) complexes with relevant tetradentate pyridine-containing macrocycles.[20,22,28–31,57]

Structural data confirm that the pendant arm's primary amino group with its weak coordination to the nickel(II) ion undergoes selective acylation, yielding four-coordinate complexes. Successful transmetallation allowed us to prepare copper(II) complexes bearing an acetylated aminopropyl substituent that remained detached from the metal under ambient conditions.

Conclusions

A series of square pyramidal nickel(II) complexes with pyridine-containing macrocycles bearing an aminopropyl pendant arm were prepared and characterized. The free macrocycles were stable, allowing for the performance of transmetallation reactions that yielded copper(II) complexes. The coordinated primary amino group on the long linker could be reversibly detached from the metal (copper(II) or nickel(II)) by protonation under mild conditions ($pK_a \approx 6$–8). Furthermore, the weakly coordinated amino group was selectively acylated, yielding four-coordinate square-planar nickel(II) and copper(II) complexes. Covalent modification of the five-coordinate complexes may be useful for attaching metallomacrocycles to biomolecules.

Experimental

General

All chemicals were of reagent grade and used as supplied without further purification. MALDI-TOF mass spectrometry was performed on a Bruker Biflex Instrument operating in positive reflectron mode using a dithranol matrix. Electrospray mass spectrometry was performed on a HP 5989B (Hewlett-Packard) Instrument in a 1 : 1 mixture of methanol and water with acetic acid. EPR spectra were obtained with a Bruker EMX spectrometer at 120 K in frozen propionitrile/2-methyltetrahydrofuran solutions (1 : 2), using DPPH as a standard. NMR spectra were recorded on a Bruker AM-300 spectrometer, IR spectra on a Mattson 1000 FTIR Spectrometer. UV-Vis spectra were obtained on a Hitachi U-2000 spectrometer (300–1100 nm). The UV-Vis spectra of solids were determined in Nujol mulls put on filter paper in absorbance mode as described elsewhere.[58] Elemental analyses were performed by Qualitative Technologies Inc. (Whitehouse, NJ).

Syntheses

Reduction of $[Ni(L1a)](ClO_4)_2$. 0.684 g (0.001 mol) of $[Ni(L1a)](ClO_4)_2$ synthesized by a previously reported procedure [11] was dissolved in 300 mL of water at ~50 °C, through the use of vigorous stirring, yielding a brick-red solution. Once cooled to room temperature the solution was then filtered to remove trace impurities. To this solution 0.874 g of $NaBH_4$ (0.023 mol) was added over a period of 10–15 min. The reaction mixture was seen to become black and precipitation of a gray solid was observed. The solution was left vigorously stirring overnight, during this time the solid re-dissolved, yielding a violet solution. The pH was then adjusted to between 8.5–9 through the addition of concentrated $HClO_4$, and the solution was rotary evaporated to dryness (water bath temperature ~30–40 °C). The complex was allowed to dry overnight under vacuum. Impurities resulting from the use of $NaBH_4$ were subsequently removed by dissolving the desired product in nitromethane and filtering off insoluble material. Yield of a mixture of $[Ni(L2a)](ClO_4)_2$ and $[Ni(L2b)](ClO_4)_2$: 0.318 g (46%).

Separation of $[Ni(L2a)](ClO_4)_2$ and $[Ni(L2b)](ClO_4)_2$. Ethanol (70 mL) was added to 0.318 g (0.6 mmol) of the isomer mixture. The suspension was stirred and brought to the boil. The mixture was then allowed to cool to room temperature and filtered, yielding a pink solution and blue solid. The solid was placed back into a flask and this process was repeated three more times. The periwinkle solid material $[Ni(L2a)](ClO_4)_2$ was then collected and washed with ether. The complex was allowed to dry overnight under vacuum. Yield of $[Ni(L2a)](ClO_4)_2$:

0.153 g (48%). Anal. found: C, 37.4; H, 5.63; N, 11.91. Calc. for $C_{16}H_{33}Cl_2N_5NiO_8$: C, 37.5; H, 5.76; N, 12.13%. ESMS: *m*/*z* 189 (NiL^+). Dissolution of the material in an ethanol–nitromethane mixture followed by ether diffusion yielded X-ray quality crystals.

All ethanol fractions were consolidated and rotary evaporated to a volume of 180 mL. This solution was placed into the refrigerator and then frozen. After 1–2 days a crystalline magenta precipitate of $[Ni(L2b)](ClO_4)_2$ formed and was collected by suction filtration. The mother liquor was concentrated and the process repeated. The complex was allowed to dry overnight under vacuum. Yield of $[Ni(L2b)](ClO_4)_2$: 0.147 g (46% yield). Anal. found: C, 37.0; H, 5.63; N, 11. 69. Calc. for $C_{16}H_{33}Cl_2N_5NiO_8$: C, 37.5; H, 5.76; N, 12.13%. ESMS: *m*/*z* 189 (NiL^+).

Dissolution of the material in acetonitrile followed by ether diffusion yielded X-ray quality crystals.

L2a. 40.4 mg (0.07 mmol) of $[Ni(L2a)](ClO_4)_2$ were dissolved in ~8.5 mL of warm water. The solution was then allowed to cool to room temperature. To this solution six equivalents (0.0206 g, 0.42 mmol) of NaCN were added and the solution instantly turned from blue to yellow. The ligand was then extracted with methylene chloride (3 × 5 mL). All methylene chloride portions were consolidated and dried over sodium sulfate overnight. The solution was concentrated to dryness yielding yellow oil. The ligand was allowed to dry overnight under vacuum. Yield: 0.018 g (80%). ^{1}H NMR ($CDCl_3$): δ 1.372 (2, 6H), 1.531–1.806 (m, 8H), 2.165–2.505 (m, 12H), 2.653 (t, 2H), 3.667 (quartet, 2H), 6.937 (d, 2H), 7.516 (t, 1H). ^{13}C NMR ($CDCl_3$): δ 24.14, 27.57, 30.53, 40.84, 45.55, 51.01, 51.70, 59.61, 120.60, 136.45, 164.46 (11 signals). MS (DIP EI): *m*/*z* 320 (L^+, 100%)

L2b. The procedure described above for L2a was applied to a magenta solution of 40.3 mg (0.07 mmol) of $[Ni(L2a)](ClO_4)_2$ in 5.5 mL of warm water, yielding 0.020 g (90%) of L2b. ^{1}H NMR ($CDCl_3$): δ 1.372 (2, 6H), 1.531–1.806 (m, 8H), 2.165–2.505 (m, 12H), 2.653 (t, 2H), 3.667 (quartet, 2H), 6.937 (d, 2H), 7.516 (t, 1H). ^{13}C NMR ($CDCl_3$): δ 24.14, 27.57, 30.53, 40.84, 45.55, 51.01, 51.70, 59.61, 120.60, 136.45, 164.46 (11 signals). MS (DIP EI): *m*/*z* 320 (L^+, 100%).

$[Cu(L2a)](ClO_4)_2$. 0.018 g (0.056 mmol) of L2a were dissolved in ~2 mL of acetonitrile and to this solution 0.9 equivalents of $Cu(ClO_4)_2{\cdot}6H_2O$ (0.0187 g, 0.050 mmol), dissolved in 1 mL of acetonitrile, was added. The acetonitrile solution instantaneously turned blue, and the solid product precipitated upon addition of ether. Yield: 0.030 g (90%). MALDI-TOF MS: 383 (CuL^+, 100%). EPR (EtCN–MeTHF): $g_{||} = 2.210$, $A_{||} = 168 \times 10^{-4}$ cm^{-1}, $g_{\perp} = 2.06$. EPR (EtCN–MeTHF + triflic acid): $g_{||} = 2.187$, $A_{||} = 196 \times 10^{-4}$ cm^{-1}, $g_{\perp} = 2.046$.

Slow ether diffusion into the acetonitrile solution of $[Cu(L2a)](ClO_4)_2$ yielded two types of crystals suitable for X-ray analysis: needle like blue crystals of $[Cu(L2a)](ClO_4)_2$, and purple crystals of $[Cu(HL2a)](ClO_4)_3{\cdot}CH_3CN$.

$[Cu(L2b)](ClO_4)_2$. The above procedure was applied to 0.020 g (0.063 mmol) of L2b, yielding 0.033 g (90%) of crystalline complex. MALDI-TOF MS: *m*/*z* 383 (CuL^+, 100%). EPR (EtCN–MeTHF): $g_{||} = 2.208$, $A_{||} = 170 \times 10^{-4}$ cm^{-1}, $g_{\perp} = 2.06$. EPR (EtCN–MeTHF + triflic acid): $g_{||} = 2.192$, $A_{||} = 193 \times 10^{-4}$ cm^{-1}, $g_{\perp} = 2.046$.

$[Ni(L1c)](ClO_4)_2$. 3.65 g (10 mmol) of $Ni(ClO_4)_2{\cdot}6H_2O$ was dissolved in 168 mL of water. This solution was added to a stirred solution of 1.883 g (10 mmol) of tris(3-aminopropyl)amine in 650 mL of water. Upon addition of the nickel salt the solution instantly changed from clear to sky blue (pH between 8–9). A solution of 1.351 g (10 mmol) diformylpyridine (synthesized by a previously reported procedure)[59] in 200 mL of ethanol was subsequently added to the mixture over a period of 20–25 minutes (the color changed from the original sky blue to a deep red) and stirring at room temperature continued for four days. The solution was then rotary evaporated to dryness, using a water bath of ~25 °C and condenser with chilled water (heating the reaction mixture resulted in decomposition of the product), and the dark red solid containing small amounts of a violet solid (determined by X-ray crystallography to be the same complex with no acetonitrile in the crystal lattice) was allowed to dry overnight under vacuum. Yield: 5.26 g (96%). Crystallization occurred by dissolving the residue in the minimum volume of acetonitrile followed by ether diffusion into the solution. The complex was allowed to dry overnight under vacuum. Found: C, 33.74; H, 5.02; N, 12.45. Calc. for $C_{16}H_{27}Cl_2N_5NiO_9$: C, 34.13; H, 4.83; N, 12.44%. IR (KBr): 1636w ($\nu_{C=N}$), 1596m, 1542m, (pyridine and NH), 1100 (br, ClO_4^-) cm^{-1}. MALDI-TOF MS: *m*/*z* 346 (NiL^+, 100%).

$[Ni(L2c)](ClO_4)_2$. 1.47 g (2.61 mmol) of $[Ni(L1c)](ClO_4)_2$ was dissolved in 500 mL of warm water and stirred. The brick-red solution was then filtered. To the stirred solution 7.11 g (0.19 mol) of $NaBH_4$ was added. During this period, the formation of a black precipitate was observed. The solution was left to stir vigorously for two days during which time the precipitate re-dissolved. To the resulting purple solution 1 g (0.027 mol) of $NaBH_4$ was added and left to sit an additional two days in order to ensure complete reduction. The pH of the solution was then adjusted to 9 with $HClO_4$ (70%). The solution was filtered and rotary evaporated to dryness. During the concentration of the solution, a fluffy brown byproduct precipitated and was periodically filtered off. The complex was allowed to dry overnight under vacuum. Nitromethane was added to the dried complex and the solution then filtered. To the concentrated solution small portions of ethanol (~5 mL) were added. The addition caused the precipitation of further impurities that were filtered off and discarded. Additional purification of the material was performed by adding diethyl ether to the nitromethane–ethanol solution. The solution was then rotary evaporated to dryness making sure the water bath temperature never exceeded 40 °C. The complex was allowed to dry overnight under vacuum. Yield: 0.62 g (45.3%). IR (KBr): ν(NH) 1612m, ν(pyridine) 1584m, $\nu(ClO_4^-)$ 1100 (br) cm^{-1}. MALDI-TOF MS: *m*/*z* 350 (NiL^+, 100%). Single crystals for X-ray diffraction analysis were obtained by ether diffusion into an acetonitrile–nitromethane (1 : 1) solution of $[Ni(L2c)](ClO_4)_2$.

L2c. The ligand was isolated in 63% yield from 39.9 mg (0.073 mmol) of $[Ni(L2c)](ClO_4)_2$ dissolved in ~5.5 mL of warm water using the procedure described above for the preparation of L2a. ^{1}H NMR ($CDCl_3$): δ 1.550 (m, 2H), 1.710 (m, 4H), 2.391 (m, 6H), 2.506 (t, 4H), 2.630 (t, 2H), 3.865 (s, 4H), 7.017 (d, 2H), 7.549 (t, 1H). ^{13}C NMR ($CDCl_3$): δ 27.42, 29.59, 40.45, 46.51, 50.38, 52.16, 54.22, 120.57, 136.51, 159.23 (10 signals). MS (DIP EI): *m*/*z* 292 (L^+, 100%)

$[Cu(L2c)](ClO_4)_2$. This complex was prepared in 90% yield from 0.013 g (0.044 mmol) of the L2c ligand dissolved in ~2 mL of acetonitrile, using the procedure described above for the preparation of $[Cu(L2a)](ClO_4)_2$. MALDI-TOF MS: *m*/*z* 354 (CuL^+, 92%). EPR (EtCN–MeTHF): $g_{||} = 2.207$, $A_{||} = 166 \times 10^{-4}$ cm^{-1}, $g_{\perp} = 2.06$. EPR (EtCN–MeTHF + triflic acid): $g_{||} = 2.191$, $A_{||} = 202 \times 10^{-4}$ cm^{-1}, $g_{\perp} = 2.044$.

$[Ni(L3c)](ClO_4)_2$. 0.104 g (0.19 mmol) of $[Ni(L2c)](ClO_4)_2$ were dissolved in 5 mL of nitromethane to which 0.5 mL of 2,6-lutidine was added followed by 0.25 mL of acetic anhydride. Upon the addition of the last reagent the solution underwent a color change from violet to orange–brown (~30 seconds). The

mixture was then rotary evaporated to dryness and the solid residue was repeatedly washed with warm toluene under vigorous stirring until the solvent remained clear. The complex was allowed to dry overnight under vacuum. Yield: 0.075 g (63%). Found: C, 37.21; H, 5.10; N, 12.15. Calc. for $C_{18}H_{31}Cl_2N_5NiO_9$: C, 36.67; H, 5.30; N, 11.89%. Dissolution of the material in acetonitrile–nitromethane (1 : 1) followed by slow ether diffusion resulted in single crystals.

L3c. 0.0389 g (0.066 mmol) of $[Ni(L3c)](ClO_4)_2$ dissolved in 10 mL of warm water. To the orange–brown solution 8 equivalents (0.026 g, 0.53 mmol) of NaCN were added. The solution turned yellow and the ligand was extracted into 15 mL of chloroform (3 × 5 mL). The extract was then dried overnight over Na_2SO_4 and rotary evaporated to dryness. The solid ligand was allowed to dry overnight under vacuum. Yield: 0.0146 g (65%). ^{1}H NMR ($CDCl_3$): δ 1.596 (m, 2H), 1.727 (m, 4H), 1.824 (s, 3H), 2.335 (t, 6H), 2.598 (t, 4H), 3.067 (m, 2H), 3.865 (s, 4H), 6.999 (d, 2H), 7.550 (t, 1H). ^{13}C NMR ($CDCl_3$): δ 24.92, 25.72, 27.80, 37.65, 47.90, 51.15, 53.36, 54.44, 120.91, 137.22, 159.37, 170.49 (12 signals). MS (DIP CI): *m*/*z* 334 (L^+, 100%).

[Cu(L3c)](ClO$_4$)$_2$. 0.0146 g (0.044 mmol) of the amine L3c was dissolved in 3 mL of ethanol. One equivalent of $Cu(ClO_4)_2\cdot 6H_2O$ (0.016 g) was dissolved in 1 mL of ethanol. Upon addition of the copper solution to that of the amine a purple precipitate formed. This precipitate was collected on a filter frit and was then washed three times with 1 mL of cold ether. Additional amounts of product were collected from the mother liqor: the ethanol purple filtrate was concentrated and placed in the freezer (−10 °C) for a few hours. The precipitate was then collected and washed with ether. The complex was allowed to dry overnight under vacuum. Combined yield: 0.0249 g (98%). X-Ray quality crystals were obtained by slow diffusion of ether into acetonitrile solution of the complex.

[Ni(L4c)](ClO$_4$)$_2$. 0.110 g (0.20 mmol) of $[Ni(L2c)](ClO_4)_2$ were dissolved in 5 mL of nitromethane to which 0.5 mL of 2,6-lutidine was added followed by 0.30 mL of benzoyl chloride. Upon addition of the last reagent the solution underwent a color change from violet to orange–brown (~30 seconds). The mixture was then rotary evaporated to dryness, and the solid residue was washed with several 5 mL portions of warm toluene upon vigorous stirring. The orange solid was then dissolved in nitromethane and precipitated out with ether yielding a tan solid. The complex was dried overnight under vacuum. Yield: 0.06 g (52%).

L4c. Free ligand L4c was isolated from 0.0430 g (0.066 mmol) of $[Ni(L4c)](ClO_4)_2$ in 65% yield, following the procedure for the preparation of L3c. ^{1}H NMR ($CDCl_3$): δ 1.721 (m, 4H), 2.375 (m, 6H), 2.679 (t, 4H), 3.199 (quartet, 2H), 3.844 (s, 4H), 6.980 (d, 2H), 7.456 (m, 3H), 7.539 (t, 1H), 7.912 (m, 2H). ^{13}C NMR ($CDCl_3$): δ 25.64, 27.36, 36.71, 48.45, 49.66, 53.84, 54.15, 120.67, 127.24, 128.76, 131.15, 135.08, 137.10, 158.92, 167.45 (15 signals). MS (DIP CI): *m*/*z* 396 (L^+, 48%).

[Cu(L4c)](ClO$_4$)$_2$. Was synthesized similarly to $[Cu(L3c)](ClO_4)_2$, starting from 0.0169 g (0.043 mmol) of the amine L4c. Crystallization from ether diffusion into a concentrated solution of the complex in acetone–acetonitrile (~19 : 1) resulted in rectangular crystals. Yield: 0.0183 g (95%). MALDI-TOF MS: *m*/*z* 359 (CuL^{2+}, 36%).

Determination of the protonation constants

The protonation constant of each complex's side arm was determined by combined spectrophotometric and pH-potentionmetric titrations. UV-Vis spectra were recorded with a Hithachi U-2000 spectrophotometer. The pH measurements were carried out with a Denver Instrument Model 250 pH-meter equipped with a glass pH/ATC electrode. The values of pK_as were easily determined from the linear graphs $\log\{(\varepsilon_{[ML]} - \varepsilon_i)/(\varepsilon_i - \varepsilon_{[M(HL)]})\}$ *vs.* pH, where $\varepsilon_{[M(L)]}$, $\varepsilon_{[M(HL)]}$, and ε_i are molar optical absorbancies of $[M(L)]^{2+}$, $[M(HL)]^{3+}$, and their mixutures during the titrations, respectively. The values of ε were corrected for dilution during the titrations. Different wavelengths were used for the calculation of pK_as and gave almost identical results. All measurements were done at 25.0 ± 0.1 °C and the ionic strength of 0.100 M (KNO_3). In a typical experiment, 3 μmol of a solid complex $[ML](ClO_4)_2$ was dissolved in 3.00 mL of 0.100 M aqueous KNO_3 solution. Nitric acid (0.200 M) was added in 10 μL portions. UV-Vis spectrum and pH of the solution were recorded after each addition. When UV-Vis spectra no longer changed (usually at pH below 3), the titration was reversed with the additions of 10 μL portions of 0.200 M aqueous KOH until the pH reached 11. The calibration of the pH-meter was periodically checked during the titration using standard buffer solutions. This procedure was tested on the $[Ni(L1a)]^{2+}$ complex and gave the value of pK_a = 6.47(3), which agrees perfectly with the value of 6.46(3) obtained form a previous independent pH-potentiometric determination.[11] The ε–pH titration curves showed a single reversible process for complexes $[Ni(L2a)]^{2+}$, $[Ni(L2b)]^{2+}$, and $[Ni(L2c)]^{2+}$ and one quasi-reversible process for $[Ni(L1c)]^{2+}$, with an inflection point around pH 6–7. Complexes $[Cu(L2a)]^{2+}$, $[Cu(L2b)]^{2+}$, and $[Cu(L2c)]^{2+}$ showed a reversible process around pH 6–7, followed by a quasi-reversible process at pH above 8, which made the determination of the pK_as for the Cu complexes less accurate. Acylated complexes $[M(L3c)]^{2+}$ and $[M(L4c)]^{2+}$ (M = Ni, Cu) showed pH-independent UV-Vis spectra up to pH 11. Above pH 11, the nickel(II) complexes with L3c and L4c were found to react with oxygen, and further titrations were carried out under nitrogen. For both nickel(II) and copper(II) complexes with acylated macrocycles, addition of base after pH 11 under nitrogen caused quasi-reversible spectral changes without saturation accompanied by the precipitation of solids. It is not clear if the spectral changes are due to the deprotonation and coordination of the pendant amide group in the complexes, or due to a decomposition process (*e.g.*, the formation of metal hydroxides).

X-Ray diffraction studies

Crystal data are summarized in Tables 4 and 5.

Data for $[Ni(L2a)](ClO_4)_2$, $[Cu(L2a)](ClO_4)_2\cdot CH_3CN$, $[Cu(HL2a)](ClO_4)_3\cdot CH_3CN$, $[Cu(L2b)](ClO_4)_2\cdot 2C_3H_6O$, and $[Cu(L3c)](ClO_4)_2$ were collected using a Bruker SMART CCD (charge coupled device) based diffractometer equipped with an LT-3 low-temperature apparatus operating at 213 K. A suitable crystal was chosen and mounted on a glass fiber using paratone oil. Data were measured using omega scans of 0.3° per frame for 30 seconds, such that a hemisphere was collected. A total of 1271 frames were collected with a maximum resolution of 0.75 Å. Data for $[Ni(L3c)](ClO_4)_2\cdot CH_3NO_2$ and $[Cu(L4c)](ClO_4)_2$ were collected at 298 K; the crystals were mounted on a glass fiber using glue. A total of 1651 frames were collected with a maximum resolution of 0.75 Å for $[Ni(L3c)](ClO_4)_2\cdot CH_3NO_2$ and 0.80 Å for $[Cu(L4c)](ClO_4)_2$. The first 50 frames were recollected at the end of data collection to monitor for decay. Cell parameters were retrieved using SMART[60] software and refined using SAINT on all observed reflections. Data reduction was performed using the SAINT[61] software which corrects for Lorentzian polarization and decay.

Single crystal intensity measurements for $[Ni(L2b)](ClO_4)_2$ and $[Ni(L2c)](ClO_4)_2$ were collected at room temperature with a Rigaku AFC5 diffractometer, using Mo-Kα radiation, graphite monochromator and $\omega/2\theta$-scans. Lattice parameters were obtained using least squares refinement of the angles of 24 reflections with $22 < 2\theta < 26°$. Psi-scan absorption correction was applied to $[Ni(L2b)](ClO_4)_2$.

Table 4 Crystallographic parameters for Ni(II) complexes

	[Ni(L2c)](ClO$_4$)$_2$	[Ni(L2a)](ClO$_4$)$_2$	[Ni(L2b)](ClO$_4$)$_2$	[Ni(L3c)](ClO$_4$)$_2$·CH$_3$NO$_2$
Formula	$C_{16}H_{29}N_5NiCl_2O_8$	$C_{18}H_{33}N_5NiCl_2O_8$	$C_{18}H_{33}N_5NiCl_2O_8$	$C_{19}H_{34}N_6NiCl_2O_{11}$
M	549.05	577.10	577.10	652.13
T/K	293(2)	213(2)	293(2)	293(2)
Crystal system	Monoclinic	Monoclinic	Triclinic	Monoclinic
Space group	$P2_1/m$ (no. 11)	$P2_1/c$ (no. 14)	$P\bar{1}$ (no. 2)	$P2_1/n$ (no. 14)
V/Å^3	1164.5(4)	4948.2(8)	1303.9(6)	2813.2(9)
a/Å	10.275(2)	18.5147(17)	9.745(3)	12.144(2)
b/Å	9.314(2)	16.5059(13)	16.107(3)	14.008(2)
c/Å	12.170(2)	16.3212(15)	8.952(3)	16.681(3)
α/°	90	90	105.17(2)	90
β/°	91.03(3)	97.227(2)	105.66(2)	97.526(4)
γ/°	90	90	88.86(2)	90
Z	2	8	2	4
μ_{calc}/mm^{-1}	1.114	1.053	0.999	0.944
N	2329	33552	3755	12559
N_{ind}	2202 (R_{int} 0.0166)	10739 (R_{int} 0.0856)	3409 (R_{int} 0.0529)	3890 (R_{int} 0.0688)
N_{obs}	1396 [$I > 2\sigma(I)$]	5244[$I > 2\sigma(I)$]	2199 [$I > 2\sigma(I)$]	2367 [$I > 2\sigma(I)$]
Final $R1$ [$I > 2\sigma(I)$]	0.0605	0.0767	0.0593	0.0581
$wR2$ (all data)	0.2038	0.2505	0.1848	0.1845

Table 5 Crystallographic parameters for Cu(II) complexes

	[Cu(HL2a)](ClO$_4$)$_3$·CH$_3$CN	[Cu(L2a)](ClO$_4$)$_2$·CH$_3$CN	[Cu(L2b)](ClO$_4$)$_2$·2C$_3$H$_6$O	[Cu(L3c)](ClO$_4$)$_2$	[Cu(L4c)](ClO$_4$)$_2$
Formula	$C_{20}H_{37}N_6CuCl_3O_{12}$	$C_{20}H_{36}N_6CuCl_2O_8$	$C_{24}H_{42}N_5CuCl_2O_{10}$	$C_{18}H_{31}N_5CuCl_2O_9$	$C_{23}H_{33}N_5CuCl_2O_9$
M	723.45	622.99	695.07	595.92	657.989
T/K	293(2)	213(2)	213(2)	193(2)	273(2)
Crystal system	Triclinic	Monoclinic	Monoclinic	Monoclinic	Triclinic
Space group	$P\bar{1}$ (no. 2)	$P2_1/n$ (no. 14)	$P2_1/c$ (no. 14)	$P2_1/n$ (no. 14)	$P\bar{1}$ (no. 2)
V/Å^3	1498.0(4)	2779(3)	3063.3(8)	2615.4(7)	1417.0(16)
a/Å	9.0975(13)	11.431(7)	16.122(2)	10.2060(17)	8.769(6)
b/Å	11.9637(17)	8.861(5)	13.595(2)	19.104(3)	11.496(8)
c/Å	13.886(2)	28.031(16)	14.548(2)	13.750(2)	15.502(11)
α/°	91.287(3)	90	90	90	69.236(14)
β/°	94.926(3)	101.766(7)	106.128(3)	102.698(3)	80.586(18)
γ/°	95.545(4)	90	90	90	76.862(19)
Z	2	4	4	4	2
μ_{calc}/mm^{-1}	1.065	1.031	0.948	1.094	1.018
N	8549	14389	15935	19047	6315
N_{ind}	5249 (R_{int} 0.0371)	4906 (R_{int} 0.0514)	5392 (R_{int} 0.0551)	6539 (R_{int} 0.0548)	3756 (R_{int} 0.1078)
N_{obs}	3983 [$I > 2\sigma(I)$]	4663 [$I > 2\sigma(I)$]	3780 [$I > 2\sigma(I)$]	3661 [$I > 2\sigma(I)$]	1540 [$I > 2\sigma(I)$]
Final $R1$ [$I > 2\sigma(I)$]	0.0640	0.0438	0.0939	0.0865	0.0756
$wR2$ (all data)	0.1849	0.1105	0.2685	0.2751	0.2166

The structures were solved by the direct method using the SHELXS-97[62] program and refined by least squares methods on F^2, SHELXL-97,[63] incorporated in SHELXTL V5.10.[64] For [Ni(L2a)](ClO$_4$)$_2$, [Cu(L3c)](ClO$_4$)$_2$, and [Cu(L2a)](ClO$_4$)$_2$·CH$_3$CN, absorption corrections were applied using SADABS[65,66] supplied by George Sheldrick. All non-hydrogen atoms are refined anisotropically. Hydrogens were calculated by geometrical methods and refined as a riding model. For [Cu(HL2a)](ClO$_4$)$_3$·CH$_3$CN, one perchlorate anion was modeled with disorder. For [Cu(L2b)](ClO$_4$)$_2$·2C$_3$H$_6$O, the carbon C17 was found to have two orientations; the perchlorate anions were also found to be disordered.

The structure of [Cu(L2a)](ClO$_4$)$_2$·CH$_3$CN was solved in the space group $P2_1/n$ (no. 14) that was identified by analysis of systematic absences. Refinement in this space group resulted in only an $R1$ of 0.22 and therefore further analysis was performed. The data suggested that the crystal was twinned and resembled space group $C222_1$. Analysis as a pseudo-merohedral twin of the monoclinic crystal, twin law −1 0 0 0 −1 0 1 0 1, resulted in an initial $R1$ of 0.0526. Final refinement with all hydrogens and the solvent molecule included gave a refined percentage of the twin to be 33.089%.

The structure of [Ni(L2c)](ClO$_4$)$_2$ was assigned to the space group $P2_1/m$ (no. 11) by analysis of systematic absences. It was solved using heavy atom methods with subsequent analysis of the resulting Fourier maps. The structure of the complex consists of two ligand moieties with the occupancy of ½ surrounding the central Ni atom that is located on the mirror plane. This rather unusual type of disorder resulted in reasonable bond lengths and angles. An attempt to solve the structure in acentric $P2_1$ resulted in a similar Fourier map showing the pseudo-mirror plane inside the complex moiety. Another, independent data set was acquired on a different crystal of the complex [Ni(L2c)](ClO$_4$)$_2$ using a Bruker SMART diffractometer with a CCD detector and yielded identical cell parameters and identical structural solution.

The crystals used for the diffraction study showed no decomposition during data collection. All drawings are done at 50% ellipsoids.

CCDC reference numbers 198022–198030.

See http://www.rsc.org/suppdata/dt/b2/b211489e/ for crystallographic data in CIF or other electronic format.

Acknowledgements

This research was supported by Tufts University (Faculty Research Award), the NSF (CHE 0111202), and the Research Corporation (RI0223). The EPR facility at Tufts was supported by the NSF (CHE 9816557), the X-ray facility at Tufts was supported by AirForce DURIP grant F49620–01–1–0242, the CCD-based X-ray diffractometer at Harvard University was purchased through NIH grant (1S10RR11937–01). The

authors thank Prof. T. E. Haas for helpful discussions and help with X-ray diffraction studies at Tufts.

References

1 P. V. Bernhardt and G. A. Lawrence, *Coord. Chem. Rev.*, 1990, **104**, 297.
2 T. A. Kaden, *Pure Appl. Chem.*, 1993, **65**, 1477.
3 K. P. Wainwright, *Coord. Chem. Rev.*, 1997, **166**, 35.
4 J. Costamagna, G. Ferraudi, B. Matsuhiro, M. Campos-Valette, J. Canales, M. Villagran, J. Vargas and M. J. Aguirre, *Coord. Chem. Rev.*, 2000, **196**, 125.
5 K. P. Wainwright, Applications of polyaza macrocycles with nitrogen-attached pendant arms, in *Advances in Inorganic Chemistry*, A. G. Sykes, ed., Academic Press, San Diego, 2001, vol. 52, pp. 293–334.
6 R. I. Haines, *Rev. Inorg. Chem.*, 2002, **21**, 165.
7 S. M. Nelson, *Pure Appl. Chem.*, 1980, **52**, 2461.
8 G. R. Newcome and V. K. Gupta, Macrocyclic pyridines, in *Pyridine and its derivatives*, Wiley, New York, 1984, pp. 447–633.
9 D. E. Fenton and P. A. Vigato, *Chem. Soc. Rev.*, 1988, **17**, 69.
10 S. R. Collinson and D. E. Fenton, *Coord. Chem. Rev.*, 1996, **148**, 19.
11 E. V. Rybak-Akimova, A. Y. Nazarenko and S. S. Silchenko, *Inorg. Chem.*, 1999, **38**, 2974.
12 H. Keypour and D. A. Stotter, *Inorg. Chim. Acta*, 1979, **33**, 149.
13 H. Keypour, S. Salehzadeh, R. G. Pritchard and R. V. Parish, *Inorg. Chem.*, 2000, **39**, 5787.
14 H. Keypour and S. Salehzadeh, *Transition Met. Chem.*, 2000, **25**, 205.
15 D. Parker, *Chem. Soc. Rev.*, 1990, **19**, 271.
16 C. J. Anderson and M. J. Welch, *Chem. Rev.*, 1999, **99**, 2219.
17 W. A. Volkert and T. J. Hoffman, *Chem. Rev.*, 1999, **99**, 2269.
18 S. J. Grant, P. Moore, H. A. A. Omar and N. W. Alcock, *J. Chem. Soc., Dalton Trans.*, 1994, 485.
19 N. W. Alcock, K. P. Balakrishnan, A. Berry, P. Moore and C. J. Reader, *J. Chem. Soc., Dalton Trans.*, 1988, 1089.
20 N. W. Alcock, P. Moore and H. A. A. Omar, *J. Chem. Soc., Dalton Trans.*, 1986, 985.
21 N. W. Alcock, K. P. Balakrishnan, P. Moore and H. A. A. Omar, *J. Chem. Soc., Dalton Trans.*, 1987, 545.
22 N. W. Alcock, P. Moore and H. A. A. Omar, *J. Chem. Soc., Dalton Trans.*, 1987, 1107.
23 N. W. Alcock, R. G. Kingston, P. Moore and C. Pierpoint, *J. Chem. Soc., Dalton Trans.*, 1984, 1937.
24 A. M. Herrera, A. V. Kalayda, J. S. Disch, A. Y. Nazarenko, R. J. Staples and E. V. Rybak-Akimova, manuscript in preparation.
25 J. Costa, R. Delgado, M. G. B. Drew and V. Felix, *J. Chem. Soc., Dalton Trans.*, 1999, 4331.
26 L. Sacconi, F. Mani and A. Bencini, in *Comprehensive Coordination Chemistry*, G. Wilkinson, R. D. Gillard and J. A. McCleverty, eds., Pergamon Press, New York, 1987, vol. 5, p. 86.
27 A. W. Addison, T. N. Rao, J. Reedijk, J. van Rijn and G. C. Verschoor, *J. Chem. Soc., Dalton Trans.*, 1984, 1349.
28 M. Di Casa, L. Fabbrizzi, M. Licchelli, A. Poggi, D. Sacchi and M. Zema, *J. Chem. Soc., Dalton Trans.*, 2001, 1671.
29 L. F. Lindoy, T. Rambusch, B. W. Skelton and A. H. White, *J. Chem. Soc., Dalton Trans.*, 2001, 1857.
30 T. H. Lu, S. F. Tung, T. Y. Chi and C. S. Chung, *Acta Crystallogr., Sect. C*, 1998, **54**, 1069.
31 V. Felix, M. J. Calhorda, J. Costa, R. Delgado, C. Brito, M. T. Duarte, T. Arcos and M. G. B. Drew, *J. Chem. Soc., Dalton Trans.*, 1996, 4543.
32 A. T. Phillip, W. Mazurek and A. T. Casey, *Aust. J. Chem.*, 1971, **24**, 501.
33 S. V. Kryatov, B. S. Mohanraj, V. V. Tarasov, O. P. Kryatova, E. V. Rybak-Akimova, B. Nuthakki, J. F. Rusling, R. J. Staples and A. N. Nazarenko, *Inorg. Chem.*, 2002, **41**, 923.
34 M. Ciampolini, *Inorg. Chem.*, 1966, **5**, 35.
35 B. F. Hoskins and F. D. Whillans, *J. Chem. Soc., Dalton Trans.*, 1975, 657.
36 R. Morassi, I. Bertini and L. Sacconi, *Coord. Chem. Rev.*, 1973, **11**, 343.
37 J. R. Hartman, R. W. Vachet and J. H. Callahan, *Inorg. Chim. Acta*, 2000, **297**, 79.
38 J. G. Gilbert, A. W. Addison and R. J. Butcher, *Inorg. Chim. Acta*, 2000, **308**, 22.
39 B. J. Hathaway, Copper, in *Comprehensive Coordination Chemistry*, G. Wilkinson, ed., Pergamon Press, Oxford, 1987, vol. 5, pp. 533–774.
40 E. V. Rybak-Akimova, A. Y. Nazarenko, L. Chen, P. W. Krieger, A. M. Herrera, V. V. Tarasov and P. D. Robinson, *Inorg. Chim. Acta*, 2001, **324**, 1.
41 T. J. Lotz and T. A. Kaden, *Helv. Chim. Acta*, 1978, **61**, 1376.
42 A. Schiegg and T. A. Kaden, *Helv. Chim. Acta*, 1990, **73**, 716.
43 P. S. Pallavacini, A. Perotti, A. Poggi, B. Seghi and L. Fabbrizzi, *J. Am. Chem. Soc.*, 1987, **109**, 5139.
44 P. V. Bernhardt and P. C. Sharpe, *Inorg. Chem.*, 2000, **39**, 4123.
45 P. S. Donnelly, J. M. Harrowfield, B. W. Skelton and A. H. White, *Inorg. Chem.*, 2000, **39**, 5817.
46 P. S. Donnelly and J. M. Harrowfield, *J. Chem. Soc., Dalton Trans.*, 2002, 906.
47 T. Koike, T. Watanabe, S. Aoki, E. Kimura and M. Shiro, *J. Am. Chem. Soc.*, 1996, **118**, 12696.
48 M. Aoki, H. Kawatani, T. Goto, E. Kimura and M. Shiro, *J. Am. Chem. Soc.*, 2001, **123**, 1123.
49 L. Fabbrizzi, F. Foti, M. Licchelli and A. Poggi, *Inorg. Chem.*, 2002, **41**, 4612.
50 R. J. Browne, D. A. Buckingham, C. R. Clark and P. A. Sutton, *Adv. Inorg. Chem.*, 2000, **49**, 307.
51 N. Mensi and S. S. Isied, *Inorg. Chem.*, 1986, **25**, 147.
52 S. S. Isied, A. Vassilian and J. M. Lyon, *J. Am. Chem. Soc.*, 1982, **104**, 3910.
53 W. Beck and R. Kramer, *Angew. Chem., Int. Ed. Engl.*, 1991, **30**, 1467.
54 R. Kramer, M. Maurus, K. Polborn, K. Sunkel, C. Robl and W. Beck, *Chem. Eur. J.*, 1996, **2**, 1518.
55 K. Haas, W. Ponikwar, H. Noth and W. Beck, *Angew. Chem., Int. Ed.*, 1998, **37**, 1086.
56 E. Kimura, T. Gotoh and M. Shiro, *Inorg. Chem.*, 2002, **41**, 3239.
57 M. G. B. Drew and S. Hollis, *Acta Crystallogr., Sect. B*, 1980, **36**, 718.
58 R. H. Lee, E. Griswold and J. Kleinberg, *Inorg. Chem.*, 1964, **3**, 1278.
59 A. L. Vance, N. W. Alcock, D. H. Busch and J. A. Heppert, *Inorg. Chem.*, 1997, **36**, 5132.
60 SMART V 5.054 (NT), Software for the CCD Detector System, Bruker Analytical X-Ray Systems, Madison, WI, 1998.
61 SAINT V 6.02 (NT), Software for the CCD Detector System, Bruker Analytical X-Ray Systems, Madison, WI, 2000.
62 G. M. Sheldrick, SHELXS-97, Program for the Solution of Crystal Structures, University of Göttingen, Germany, 1997.
63 G. M. Sheldrick, SHELXL-97, Program for the Refinement of Crystal Structures, University of Göttingen, Germany, 1997.
64 SHELXTL 5.10 (PC-Version), Program library for Structure Solution and Molecular Graphics, Bruker Analytical X-Ray Systems, Madison, WI, 1998.
65 SADABS, Program for absorption corrections using Siemens CCD based on the methods of Robert Blessing (see ref. 66).
66 R. H. Blessing, *Acta Crystallogr., Sect. A*, 1995, **51**, 33.
67 M. N. Burnett and C. K. Johnson, ORTEP-III: Oak Ridge Thermal Ellipsoid Plot Program for Crystal Structure Illustrations, Report ORNL-6895, Oak Ridge National Laboratory, Oak Ridge, TN, USA, 1996.